Korean J. Chem. Eng., **24**(3), 481-488 (2007)

Mass transfer and reaction process of the wet desulfurization reactor with falling film by cross-flow scrubbing

Juncong Sai†, Shaohua Wu, Rui Xu, Rui Sun, Yan Zhao and Yukun Qin

School of Energy Science and Engineering, Harbin Institute of Technology, Harbin 150001, P. R. China
(*Received 22 August 2006 • accepted 6 November 2006*)

Abstract–In the present study, a series of wet flue gas desulfurization experiments have been carried out in comparison with different slurry feeding ways, i.e., by series connection and by parallel connection, by means of cross-flow scrubbing with falling film. The experiment results show that there is optimal desulfurization performance for the slurry feeding way by series connection. A liquid side mass transfer-reaction model and desulfurization mass transfer by cross-flow scrubbing model have been developed. The pH values of the outlet slurry inside the reactor and the ion concentration distributions of H_2SO_3, HSO_3^- and SO_3^{2-} along the axial direction of the tubes were obtained by analyzing and calculating the models. The calculation values agree well with the experimental values. It shows that the models can predict well the ion concentration distributions along the axial direction of the tubes.

Key words: Cross-flow Scrubbing, Falling Film, Mass Transfer-reaction Process

INTRODUCTION

As installed capacities are increased with rapid pace of economic development, the emission of sulfur dioxide (SO_2) is increased [1]. Flue gas desulfurization (FGD) is one of the most effective ways of controlling SO_2, among which wet flue gas desulfurization (WFGD) is the most widely used and developed FGD technology [2,3]. Two gas-liquid contacting ways, countercurrent flow and cocurrent flow, are applied in the conventional falling film reactors, while the contacting way of the cross flow between falling film and flue gas, as well as the liquid side mass transfer and reaction process has not been studied [4-10].

This paper originally presents the WFGD reactor with falling film by cross-flow scrubbing and studies the mass transfer and reaction process. The finned tubes are used as the carrier of falling film in the reactor to ensure uniformity, continuity, stabilization and unbrokenness.

EXPERIMENTAL PRINCIPLE AND METHOD

1. Experimental Principle

The operating principle of the flue gas crossing the finned-tube bundles is shown in Fig. 1. Lime slurry is used in the experiments as the absorbent. The slurry is distributed, by the slurry distributor, onto the guiding tubes with orderly array. Therefore, the slurry falls down along the outside surface of the tubes with the form of uniform falling film (as shown in Fig. 1 by the section plane parts). The falling film on the finned tubes is scrubbed by the cross flue gas with certain velocity, while the SO_2 is absorbed by the falling film. Thus the aim of removing SO_2 is achieved.

The falling film can cover the surface of the whole tube and not be broken easily by the flue gas because of the surface energy and the attaching area, caused by the fins of the tubes. Therefore, the entrained liquid drops can be lessened, and then the erosion problem of the back equipment can be alleviated.

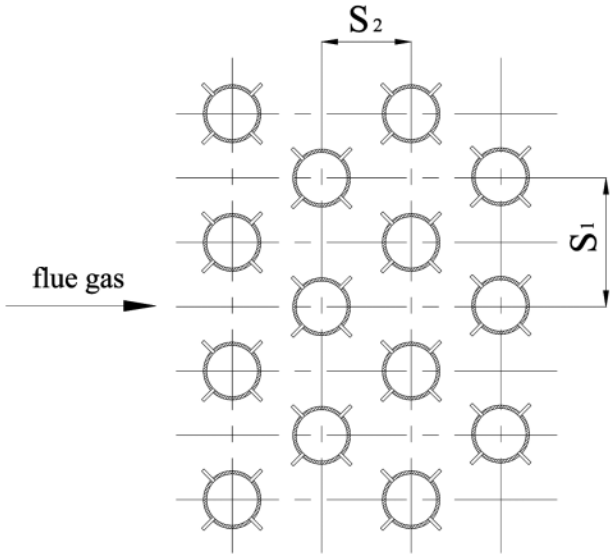

Fig. 1. Schematic illustration of flue gas crossing the finned-tube bundles.

The experiment was carried out on a test-rig. The finned-tube is the core part of the experimental system. The outside diameter and the effective length of the finned-tube are 16 mm and 500 mm, respectively. The height of the fin is 5 mm. The inside diameter of the orifice of the distributor is 18 mm. The range of the inlet flue gas temperature is from 28 °C to 100 °C. The range of the inlet flue gas velocity is from 2.4 m/s to 4.9 m/s. The range of the slurry flow rate is from 6 m^3/h to 8 m^3/h. When the flue gas velocity and the flue gas temperature at inlet are maintained at 3.2 m/s and 60 °C, respectively, the experiments are conducted with the slurry rates of

†To whom correspondence should be addressed.
E-mail: saijc@hit.edu.cn
‡This work was presented at the 6th Korea-China Workshop on Clean Energy Technology held at Busan, Korea, July 4-7, 2006.

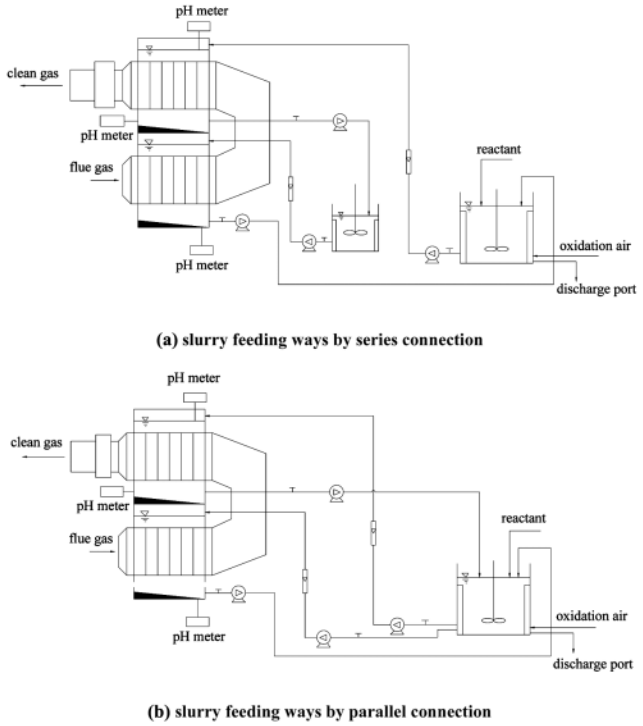

Fig. 2. Schematic illustration of the dual-loop wet FGD experimental system with the falling film.

6 m^3/h, 7 m^3/h and 8 m^3/h.

2. Experimental Method

The desulfurization experimental system comprises four subsystems: flue gas system, slurry-loop system, oxidation and blow-down system, and lime slurry feeding system. This paper presents two slurry feeding schemes as shown in Fig. 2, which are based on a different slurry feeding process: slurry feeding ways by series connection and by parallel connection. For the operating condition of the slurry feeding way by series connection, the quantity of the feeding slurry is half of that by parallel connection, that is, the liquid-gas ratio by series connection is half of that by parallel connection with the same flue gas flow rate.

EXPERIMENTAL RESULTS AND DISCUSSION

First, dual-loop WFGD experiments with falling film were conducted on the test rig with slurry feeding way by series connection (as shown in Fig. 2a). Then a series of experiments were carried out to compare the slurry feeding ways by series connection with the one by parallel connection.

1. Effect of Flue Gas Temperature and Velocity at Inlet on Desulfurization Efficiency

Fig. 3 indicates that the desulfurization efficiency increases first as the increase of gas temperature at the inlet. When the temperature reaches to about 60 °C, the maximum efficiency is obtained. Then the efficiency decreases with the increase of gas temperature. On one hand, the slurry temperature increases with the increase of flue gas temperature based on the gas-liquid balance principle. The solubility of SO_2 and $Ca(OH)_2$ decreases with the increase of slurry temperature, which will cause a decrease of the efficiency. On the other hand, the diffusion coefficients of the ions in the liquid increase with the increase of slurry temperature, and then the absorption of SO_2 is enhanced. Thus, it can be seen that the flue gas temperature is not an independent factor. Generally, the range of the inlet flue gas temperature is 59-60 °C [11].

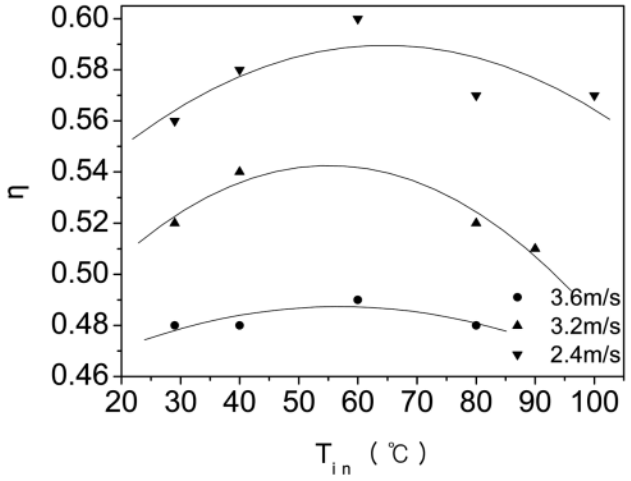

Fig. 3. Effect of the temperature of the inlet flue gas on the desulfurization efficiency.

The illustration also shows that there is a downward trend for desulfurization efficiency as the increase of the flue gas velocity at the inlet. On one hand, the gas-liquid mass transfer was enhanced with the increase of the flue gas velocity. Turbulent flow was formed on the falling film, which makes the flue gas and falling film mix well. On the other hand, the staying time of the flue gas in the reactor reduces with the increase of the flue gas, which reduces the efficiency. For this case, the staying time of the flue gas is the dominant factor.

2. Effect of SO_2 Concentration of Flue Gas at Inlet on Desulfurization Efficiency

Fig. 4 shows that the desulfurization efficiency decreases with the increase of the SO_2 concentration of flue gas at inlet. As the SO_2

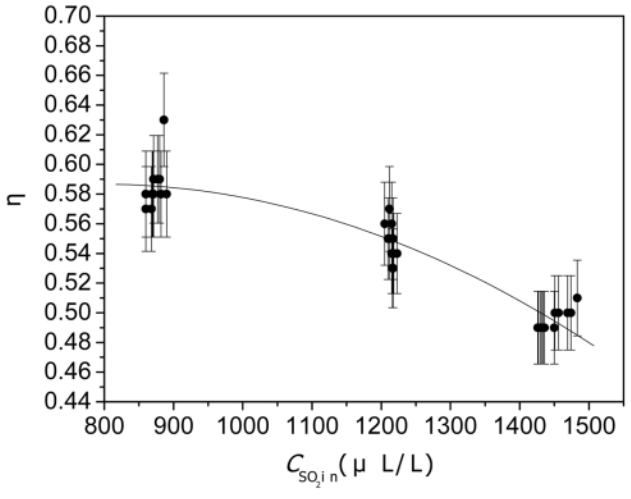

Fig. 4. Effect of the inlet SO_2 concentration on the desulfurization efficiency.

Table 1. Effect of the inlet SO_2 concentration on the desulfurization efficiency and the absorption rate

C_{in} (mg/Nm^3)	2499.64	3472.04	4135.56
η	0.585	0.549	0.496
V_{SO_2} (mg/s)	421.40	549.00	590.38

partial pressure increases with the increase of the SO_2 concentration, the mass transfer resistance can be reduced and the chemical absorption can be enhanced according to the mass transfer kinetics. However, the absorption capacity can easily reach the maximum value when the SO_2 concentration gets higher, which causes relatively less total SO_2 absorption capacity.

The following equation can be obtained by regressing the curve in Fig. 4:

$$\eta = 0.45055 + 3.42251\times10^{-4}C_{in} - 2.15101\times10^{-7}C_{in}^2 \quad (1)$$

Then the absorption rate of the slurry for the different C_{in} can be expressed as:

$$V_{SO_2} = QC_{in}\eta = V_{in}A_{in}C_{in}\eta \quad (2)$$

That is,

$$V_{SO_2} = 3.2\times0.09\times(0.45055C_{in} + 3.42251\times10^{-4}C_{in}^2 - 2.15101\times10^{-7}C_{in}^3) \quad (3)$$

where, V_{in} is equal to 3.2 m/s, and A_{in} is equal to 0.09 m^2.

The desulfurization efficiency η and the absorption rate of the slurry V_{SO_2} can be obtained from Eq. (3). The results are listed in Table 1.

It is shown that although the desulfurization efficiency η decreases with the increase of SO_2 concentration at inlet, the absorption rate V_{SO_2} increases with that. It can be explained by the following qualitative analysis.

$$V_{SO_2} = NA_{in} = K(C_{in} - C_0)A_{in} \quad (4)$$

For qualitative analysis, it can be considered that C_0=0. Therefore Eq. (4) can be simplified as:

$$V_{SO_2} = NA_{in} = KC_{in}A_{in} \quad (5)$$

Eq. (6) can be obtained by substituting Eq. (2) into Eq. (5):

$$K = \eta\left(\frac{Q}{A_{in}}\right) \quad (6)$$

When the experiment condition is fixed, (Q/A_{in}) is a constant. Therefore, it can be approximately considered that K is proportional to η, that is:

$$K \propto \eta \quad (7)$$

Based on Eq. (7), the change of η represents the change of K. It can also be seen from Fig. 4 and Table 1 that if the partial pressure of SO_2 increases with the increase of the SO_2 concentration at the inlet, it causes the reaction surface to move from the gas-liquid phase surface to the liquid-solid phase. Therefore, the total reaction rate changes from the gas control to the liquid control, which leads to the decrease of K and η.

On the other hand, it can be seen from Eq. (4) that with the increase of SO_2 concentration at the inlet, the driving force $(C_{in} - C_0)$ increases. However, K decreases to a certain extent with the increase of the SO_2 concentration at the inlet. According to Eq. (4), V_{SO_2} is proportional to K and $(C - C_0)$. As a whole, therefore, the increase of the driving force $(C_{in} - C_0)$ dominates the mass transfer process, and V_{SO_2} increases with the increase of C_{in}, which can be demonstrated by results listed in Table 1.

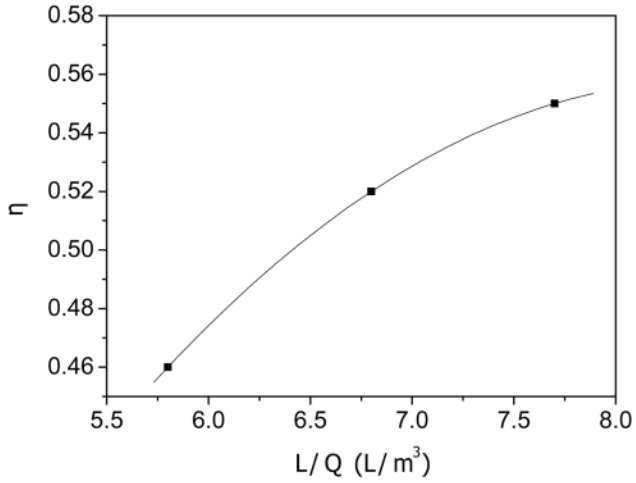

Fig. 5. Effect of the liquid-gas rate on the desulfurization efficiency.

3. Effect of Gas-liquid Ratio on Desulfurization Efficiency

The experiment results are shown in Fig. 5. The desulfurization efficiency increases with the increase of L/Q. The reasons are as follows: the thickness of the falling film increases, which expands the gas-liquid contacting area, with the increase of the slurry rate. This causes an increase of the mass transfer rate. Meanwhile, the temperature inside the tower reduces with the increase of the slurry rate, which enhances the SO_2 dissolution and decreases the mass transfer resistance in the liquid side.

4. Experimental Comparison of Slurry Feeding Ways by Series Connection and Parallel Connection

The slurry feeding rate is 7 m^3/h by series connection while that is 14 m^3/h by parallel connection (as shown in Fig. 2b). The exper-

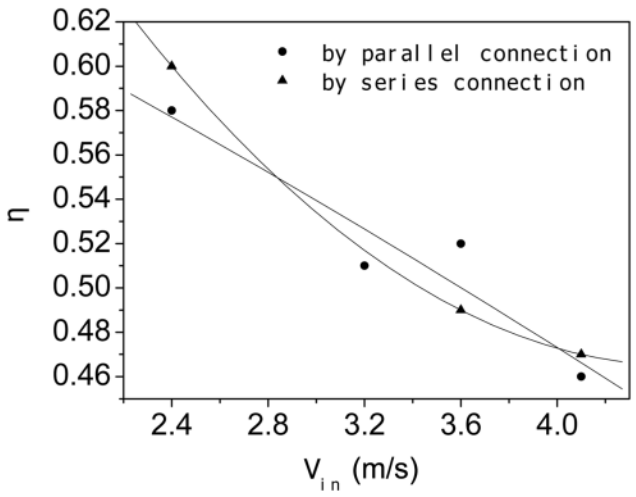

Fig. 6. Comparison of the two experimental schemes at a different velocity of the inlet flue gas.

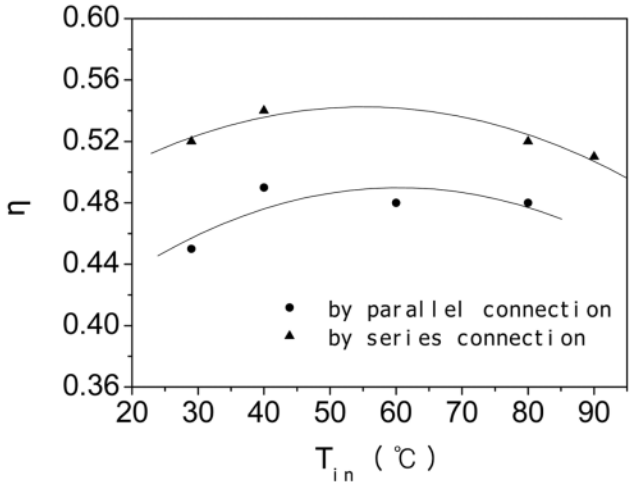

Fig. 7. Comparison of the two experimental schemes at different temperature of the inlet flue gas.

imental results are presented in Fig. 6. It can be seen from Fig. 6 that for the two ways the desulfurization efficiency decreases with the increase of the flue gas velocity at the inlet. The difference between the two schemes is not obvious, which indicates that desulfurization performance for the two ways is approximately the same. It shows that not only can the slurry feeding way by series connection fulfill the demand of removing SO_2, but also lower the gas-liquid ratio, which reduces the cost of the investment and operating cost.

Fig. 7 indicates that changing trends for the two connection ways are basically the same, that is, with the increase of the flue gas temperature at the inlet, the desulfurization efficiency increases to the maximum at a temperature of 60 °C, then the desulfurization efficiency decreases. The results agree well with those in Fig. 3. It can also be seen from Fig. 7 that for the same flue gas temperature at the inlet, the desulfurization efficiency with the slurry feeding by series connection is a little higher than that by parallel connection. The comparison of the two slurry feeding ways in Fig. 2 shows that for the same flue gas rate, the gas-liquid rate by series connection is half of that by parallel connection, but the slurry content holding in the tower is the same. As the residence time of the feeding slurry by parallel connection is half of that by series connection, most lime fed to the system can hardly dissolve. Furthermore, it can be seen from Fig. 2 that there is a stirrer in the middle circulating tank, which helps to stir and oxidize the $CaSO_3$ produced from the upper tower and enhance the mixture and reaction of the reactants and the products and increase the desulfurization efficiency. Therefore, there is the possibility to reduce the gas-liquid ratio, and, as a result, the desulfurization efficiency by series connection may be larger than that by parallel connection, just as shown in Fig. 7.

STUDY ON LIQUID SIDE MASS TRANSFER AND REACTION PROCESS

1. Setting up of Liquid Side Mass Transfer and Reaction Model

It is considered that the reaction that SO_2 reacts with $Ca(OH)_2$ slurry is irreversible and instant. The reaction between SO_2 and Ca

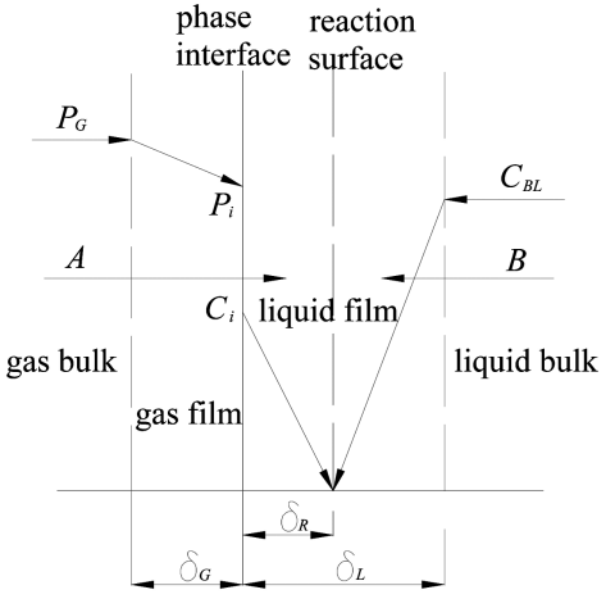

Fig. 8. Schematic illustration of the concentration distribution for the irreversible instantaneous reaction.

$(OH)_2$ slurry only happens within the liquid film. Therefore, the total reaction process shows that SO_2 reacts with $Ca(OH)_2$ to form $CaSO_3$ [12,13]. As shown in Fig. 8, the mass transfer rate from SO_2 gas to liquid bulk, based on the two film theory, can be expressed as:

$$N=k_G(P_G-P_i) \tag{8}$$

The phase equilibrium correlation is met at the phase interface:

$$C_i=HP_i \tag{9}$$

The mass transfer rate from SO_2 gas to liquid bulk can be expressed as by the liquid parameters:

$$N=k_L'C_i=Ek_LC_i \tag{10}$$

The enhancement factor E can be expressed as:

$$E=1+\frac{rC_{BL}}{bC_i} \tag{11}$$

The mass transfer rate from SO_2 gas to liquid bulk is obtained by eliminating the unknown variable according to Eqs. (8)-(11):

$$N=\frac{HP_G+\frac{rC_{BL}}{b}}{\frac{H}{k_G}+\frac{1}{k_L}} \tag{12}$$

Therefore, the mass transfer rate equation is set up while the irreversible and instant reaction happens between SO_2 gas and liquid bulk.

2. Setting up of Desulfurization Mass Transfer Model with Falling Film by Cross-flow Scrubbing

The desulfurization mass transfer model with falling film by cross-flow scrubbing studied in this paper is shown in Fig. 9, where the falling film is shown by the hatching and the fins are not shown in the planform. In order to study the mass transfer process by cross-flow scrubbing, it is assumed that:

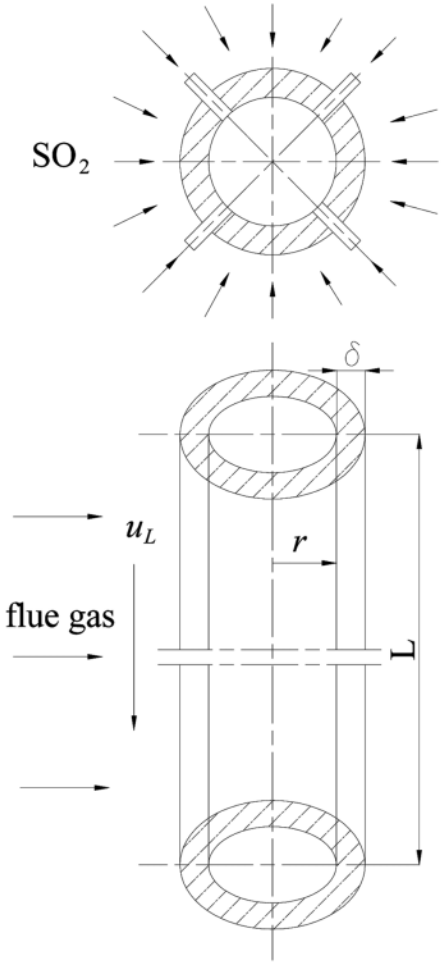

Fig. 9. Schematic illustration of the mass transfer model for the desulfurization process.

(1) The gas phase and the liquid phase both are continuum phases.

(2) The flue gas can touch the falling film fully around the tube, and the absorbing ability is the same for the falling film in each direction.

(3) The falling film can be distributed uniformly along the axis of the tube and not be broken.

(4) The mass transfer rate is invariable along the axial direction of the tube.

(5) The pH value of the inlet slurry is held at 9 during the desulfurization process.

The staying time of falling film along the tube is:

$$t = \frac{L}{u_L} \tag{13}$$

Therefore, the total molar mass of SO_2 absorbed by falling film within t is:

$$Q = NAt \tag{14}$$

The slurry bulk for absorbing SO_2 within t is:

$$V = A' u_L t \tag{15}$$

As a result, the molar concentration of absorbed SO_2 within t can be expressed as:

$$M' = \frac{Q}{V} = \frac{NAt}{A' u_L t} = \frac{NA}{A' u_L} = \frac{N \cdot [2\pi(r+\delta) - 4 \times 0.001] \cdot L}{u_L \cdot \{\pi[(r+\delta)^2 - r^2] - 4 \times 0.001 \times \delta\}} \tag{16}$$

The products from the reaction between SO_2 and $Ca(OH)_2$ slurry in the falling film exist mainly as three kinds of compounds of sulfur with 4 valence, namely $SO_{2(aq)}$, HSO_3^- and SO_3^{2-}. The total concentration of products can be expressed as:

$$M = [SO_{2(aq)}] + [HSO_3^-] + [SO_3^{2-}] \tag{17}$$

The electroneutrality equation can be used for the slurry:

$$[H^+] + 2[Ca^{2+}]_0 = [OH^-] + [HSO_3^-] + 2[SO_3^{2-}] \tag{18}$$

It is assumed that the original pH value of $Ca(OH)_2$ solution is pH_0. According to the ionization equilibrium of H_2SO_3, the absorbing equation of $Ca(OH)_2$ slurry and certain SO_2 is obtained:

$$K_w/[H^+]_0 - [H^+]_0 + [H^+] = K_w/[H^+] + \frac{MK_{S_1}(2K_{S_2} + [H^+])}{K_{S_1}K_{S_2} + K_{S_1}[H^+] + [H^+]^2} \tag{19}$$

The variable M can be separated from Eq. (18), Eq. (18) can be simplified as:

$$M = \left\{ K_w\left(\frac{1}{[H^+]_0} - \frac{1}{[H^+]}\right) + [H^+] - [H^+]_0 \right\} \frac{K_{S_1}K_{S_2} + K_{S_1}[H^+] + [H^+]^2}{K_{S_1}(2K_{S_2} + [H^+])} \tag{20}$$

Therefore, the correlation of $M' = 10^3 M$ can be obtained based on the mass conservation. Attention: the purpose of multiplying 10^3 is to unify the molar unit.

According to above analysis, it is known that hydrogen ion concentration $[H^+]$, namely pH value of the solution, can be solved by SO_2 mass transfer rate.

3. Calculation Results and Analysis

3-1. Determination of Calculation Condition

The desulfurization test rig with falling film by cross-flow scrubbing was set up. The setting conditions are these: the effective height of falling film is 0.5 m, the temperature of the inlet flue gas is 30 °C, and the velocity of the inlet flue gas is 3.2 m/s. By the experimental measurement, the average SO_2 concentration at inlet C_{in} is 1,058 μL/L and the average SO_2 concentration at outlet C_{out} is 583 μL/L, the slurry temperature is 30 °C, and the original pH value of $Ca(OH)_2$

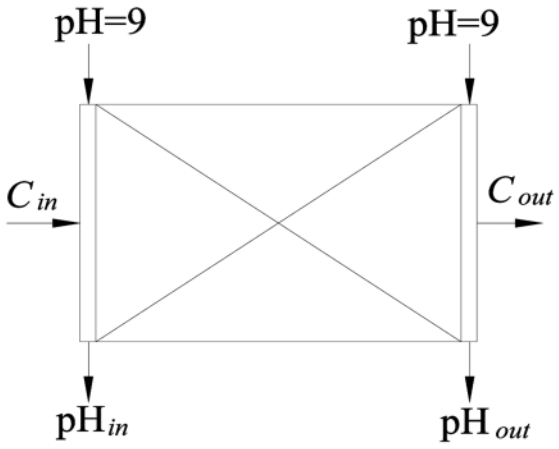

Fig. 10. The illustration of the model of the desulfurization reactor.

slurry is 9.00. The reactor model is shown in Fig. 10. The pH values of the first and the last row tubes inside the reactor are studied separately. The average values of the inlet value and the outlet value along the tubes are used as the calculation values.

3-2. Calculation Results and Error Analysis

During the calculation process, the concentration of liquid bulk of $Ca(OH)_2$ is a variable parameter. The pH value of the inlet slurry is held at 9, and the pH value of the outlet slurry is the required $[H^+]$. Therefore, the C_{BL} can be solved based on the ionization equilibrium equations of $Ca(OH)_2$ and H_2O:

$$C_{BL}=\frac{1.45\times10^{-14}}{10^{-9}+[H^+]}\ (\mathrm{mol/L}) \tag{21}$$

The outlet pH values at the first and the last row tubes can be calculated by solving Eqs. (12), (20) and (21), based on the correlation of $M'=10^3$ M and the calculation using software of MATLAB and EXCEL.

The pH value of the slurry bulk in the reactor can be calculated by averaging the outlet pH values at the first and the last row tubes:

$$\mathrm{pH}=\frac{\mathrm{pH}_{in}+\mathrm{pH}_{out}}{2}=\frac{4.71+5.35}{2}=5.03$$

The calculated pH value is a little lower than the measured one ($pH_{measure}$=6.06). By analysis, the errors are caused by the following reasons:

3-2-1. Measurement errors.

An acidimeter of PHS-2C type is used for monitoring the pH value of the slurry during the experimental process. The acidimeter is suitable for measuring the pH value of water with little solid substance. There are some solid substances (mainly the undissolved $Ca(OH)_2$, the formed $CaSO_3$, and the additive $CaSO_4$). The glass ball of the electrode probe is liable to contaminating and plugging and leads to the passivation of the probe and reducing sensitivity, which causes the numerical reading inaccuracy. Therefore, the acidimeter must be calibrated before the experiment so as to reduce the error from the numerical reading.

3-2-2. Idealization of the model assumption.

The practical situation is not like the No. 2 and 3 assumptions for setting the mass transfer model. It is observed that the falling film can expand and cover the fins and is broken, and there is a reversed-flow region at the leeward side of the tube, where the mass transfer rate is little. It is shown by the experimental results that the falling film shape can affect the desulfurization efficiency. Therefore, the above will cause the SO_2 absorption rate to increase and the outlet pH value of the slurry to reduce.

3-2-3. Determination of the bulk concentration of $Ca(OH)_2$.

In this paper the bulk concentration of $Ca(OH)_2$ is obtained based on the ionization equilibrium equations of $Ca(OH)_2$ and H_2O. But the way for determining the bulk concentration of $Ca(OH)_2$ is inaccurate, and the bulk concentration of $Ca(OH)_2$ changes with the reaction carrying out. The No. 4 assumption of the mass transfer model is also idealized, for the mass transfer rate changes with the C_{BL} changing along the height of the tube. This is one of the reasons for causing the error.

3-2-4. Selection of the calculation formulae.

Some empirical equations and correlation formulae are used during the calculation process. This is also one of the reasons for causing the error.

Furthermore, another operating condition was solved. The setting conditions are these: the effective height of falling film is 1.0 m, the temperature of the inlet flue gas is 30 °C, and the velocity of the inlet flue gas is 3.2 m/s. By the experimental measurement, the average SO_2 concentration at inlet C_{in} is 1058 μL/L and the average SO_2 concentration at outlet C_{out} is 516 mL/L, the slurry temperature is 30 °C, and the original pH value of $Ca(OH)_2$ slurry is 9.02.

The pH value of the slurry bulk in the reactor can be calculated as follows:

$$\mathrm{pH}=\frac{\mathrm{pH}_{in}+\mathrm{pH}_{out}}{2}=\frac{4.48+5.07}{2}=4.78$$

The calculated pH value is also a little lower than the measured one ($pH_{measure}$=5.52).

According to the above analysis, the calculating model is an effective way for studying the liquid side mass transfer and reaction process of the falling film, though the calculated results are a little lower than the measured ones. These results will offer the design and optimization the theoretical supports for the reactor by cross-flow scrubbing.

3-3. Distributions of Ion Concentration Along the Height of the Tubes

The slurry pH values at the first and the last row tubes and the ion concentration distributions of H_2SO_3, HSO_3^- and SO_3^{2-} along the height of the tubes can be obtained based on the above deduction and the ionization equilibrium equations of H_2SO_3 when the effective height of the falling film is 0.5 m, as shown in Fig. 11-14.

Fig. 11 shows that the pH value reduces with the increase of the distance along the flowing direction of the falling film. The slurry pH value at the inlet decreases sharply at the beginning, then tends towards smoothly while L is larger than 0.25 m. The slurry pH value at the outlet changes smoothly at the beginning, then decreases quickly while L is larger than 0.15 m. The slurry can absorb SO_2 quickly and the slurry pH value reaches to 5.2 at the position of 0.25 m because the SO_2 concentration at the inlet is higher and the mass transfer rate is invariable along the axis of the tube. The mass transfer process is controlled by the liquid side and thus the slurry pH value

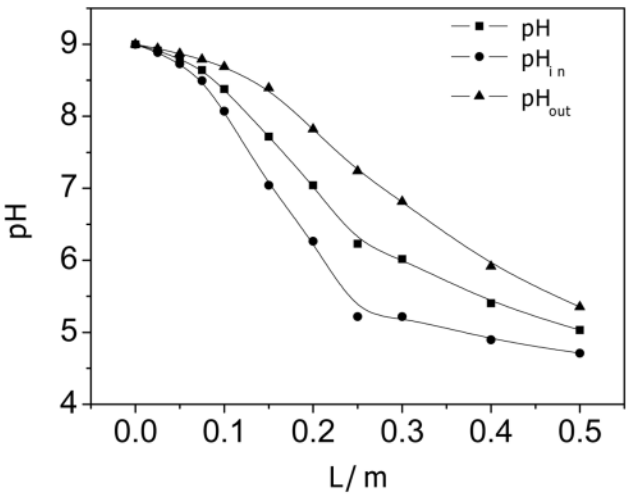

Fig. 11. The change of the pH value along the height of the tube.

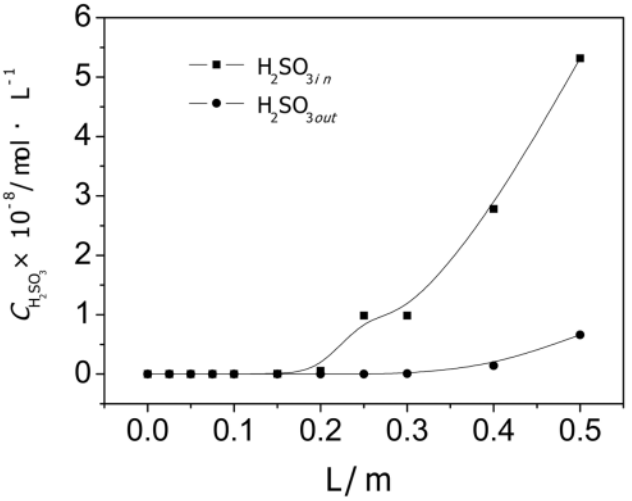

Fig. 12. The change of H_2SO_3 concentration along the height of the tube.

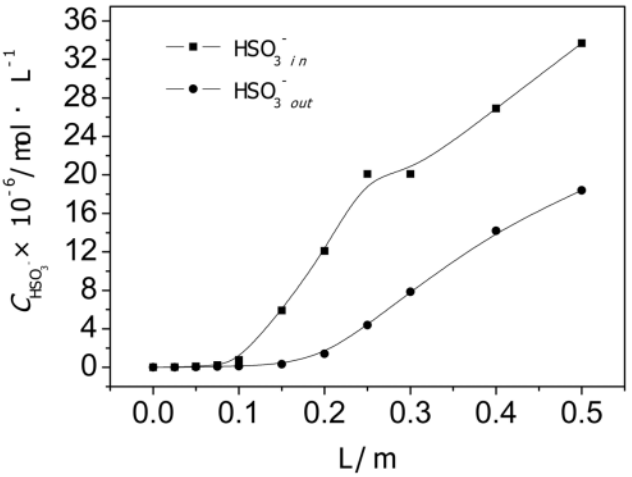

Fig. 13. The change of HSO_3^- concentration along the height of the tube.

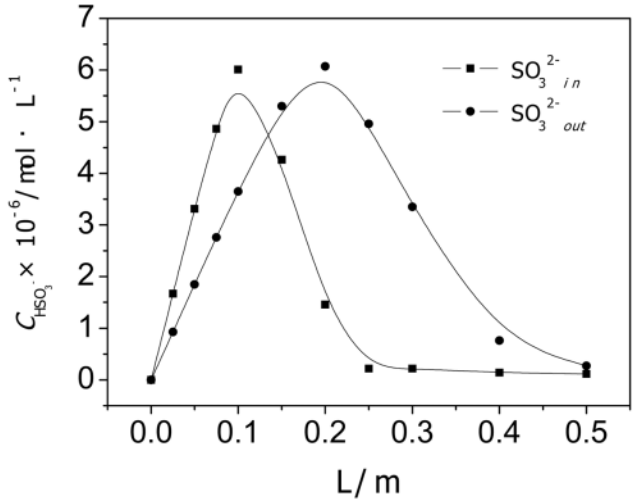

Fig. 14. The change of SO_3^{2-} concentration along the height of the tube.

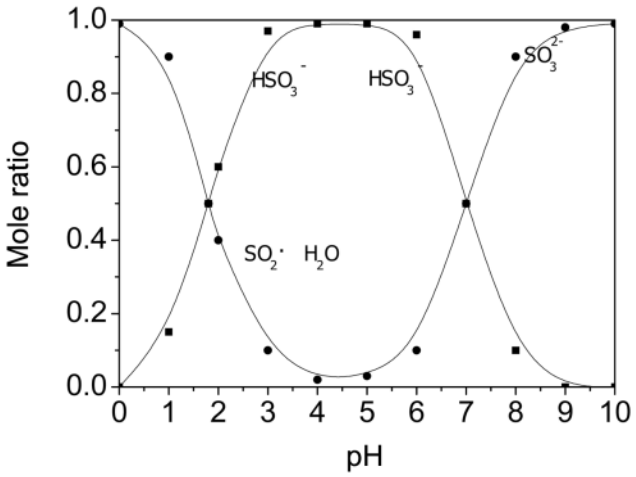

Fig. 15. Effect of the slurry pH value on S^{IV} mole ratio (25 °C).

changes smoothly. The slurry at the outlet can absorb more SO_2 for the lower SO_2 concentration at the outlet. Therefore the slurry pH value will decrease sharply at a position of 0.15 m.

Fig. 11 to 14 indicates in comparison with Fig. 15 that:

The ion concentration of H_2SO_3, and HSO_3^- in the slurry increases and the ion concentration of SO_3^{2-} increases then reduces with the increase of the distance along the flowing direction of the falling film at either the inlet or outlet.

For the inlet of the reactor, namely the first row tubes, the pH value is larger than 6.26 with little formed H_2SO_3 when L is less than 0.2 m. The concentration of the formed H_2SO_3 increases with the decrease of the pH value. For HSO_3^-, a little HSO_3^- exists when the reaction happens. The concentration of HSO_3^- tends towards a maximum when the pH value is under 5.21, namely L is larger than 0.3 m. For SO_3^{2-}, the pH value is larger than 8.07 when L is less than 0.1 m. The concentration of SO_3^{2-} increases from zero to maximum (namely, the corresponding value when L is equal to 0.1 m) quickly with the reaction process. The substance in the slurry is almost SO_3^{2-}. The concentration of SO_3^{2-} reduces to a minimum point when L is equal to 0.25 m and the slurry pH value reduces to 5.22, then tends towards smoothly with the decrease of pH value.

For the outlet of the reactor, namely the last row tubes, the pH value is larger than 8.35 with little formed H_2SO_3 when L is less than 0.4 m. The concentration of the formed H_2SO_3 increases little with the sharp decrease of the pH value. For HSO_3^-, a little HSO_3^- has existed when the reaction happens. The concentration of HSO_3^- tends towards the maximum when the pH value is under 5.35, namely L is larger than 0.4 m. For SO_3^{2-}, the pH value is larger than 8.39 when L is less than 0.15 m. The concentration of SO_3^{2-} increases from zero to maximum (namely the corresponding value when L is equal to 0.2 m) quickly with the reaction process. The substance in the slurry is almost SO_3^{2-}. The concentration of SO_3^{2-} reduces to minimum point quickly with the reduction of the slurry pH value.

It can be seen from the order of magnitude of the product in the figure that the formed quantity of H_2SO_3 is little. It shows that the absorbed SO_2 reacts with $Ca(OH)_2$ completely. At the position with the same height, the concentrations of HSO_3^- and SO_3^{2-} at the inlet

are higher than at the outlet because of the higher inlet SO_2 concentration.

CONCLUSIONS

1. For the slurry feeding ways by series connection: the desulfurization efficiency increases first with the increase of the temperature of the inlet flue gas. The desulfurization efficiency reaches a maximum value when the temperature of the inlet flue gas reaches 60 °C. Then the desulfurization efficiency decreases with the increase of the temperature of the inlet flue gas. The desulfurization efficiency decreases with the increase of the velocity of the inlet flue gas. The desulfurization efficiency decreases with the increase of the inlet SO_2 concentration. The desulfurization efficiency increases with the increase of the liquid-gas ratio.

2. A comparison of the experimental results of the two slurry feeding ways shows that there is optimal desulfurization performance for the slurry feeding way by series connection, characterized with the high desulfurization efficiency and the low liquid-gas ratio, which is lower than that of conventional WFGD equipment. This slurry feeding way can reduce the investment and the operating cost of the equipment.

3. A liquid side mass transfer-reaction model and desulfurization mass transfer by cross-flow scrubbing model have been developed. The pH value of the outlet slurry of the reactor at the effective height of 0.5 m and 1.0 m, respectively, was obtained from the calculation results. Though this value is a little lower than the experimental value, the model is also an effective calculation way for the liquid side mass transfer-reaction process. The causes of errors were analyzed.

4. The pH values of the outlet slurry inside the reactor and the ion concentration distributions of H_2SO_3, HSO_3^- and SO_3^{2-} along the axial direction of the tubes were obtained by analyzing and calculating the models. These results will offer theoretical support for the design and optimization of the reactor by cross-flow scrubbing.

NOMENCLATURE

A : effective surface area of liquid film for absorbing SO_2 gas [m^2]; species A
A_{in} : cross-section area of reactor at inlet [m^2]
A' : effective cross-section area of falling film [m^2]
B : species B
b : stoichiometric coefficient
C : ion concentration [mol/L]
C_0 : concentration of species A in liquid bulk [mol/m^3]
C_{BL} : concentration of liquid bulk [mol/L]
C_i : concentration of A at phase interface [mol/m^3]
C_{in} : average SO_2 concentration at inlet [μL/L]
C_{out} : average SO_2 concentration at outlet [μL/L]
E : enhancement factor
H : solubility coefficient [mol/(m^3-Pa)]
K : convection mass transfer coefficient based on concentration difference of ($C_{in} - C_0$) [m/s]
K_{S_1} : first-order dissociation constant of H_2SO_3 [mol/L]
K_{S_2} : second-order dissociation constant of H_2SO_3 [mol/L]
K_w : dissociation constant of water [mol^2/dm^6]
k_G : gas side mass transfer coefficient [mol/(m^2-s-Pa)]
k_L : liquid side physical mass transfer coefficient [m/s]
k'_L : liquid side chemical mass transfer coefficient [m/s]
L : effective height of finned tube [m]
M : molar concentration of sulfur element of +4 valence in solution [mol/L]
M′ : molar concentration of sulfur dioxide absorbed by falling film [mol/m^3]
N : absorption rate [mol/(m^2-s)]
P_G : partial pressure of species A in gas bulk [Pa]
P_i : partial pressure of species A at phase interface [Pa]
pH_{in} : pH value of inlet slurry at inlet of reactor
pH_{out} : pH value of outlet slurry at outlet of reactor
Q : molar mass of sulfur dioxide absorbed by falling film [mol]
r : radius of tube, m; diffusion coefficient ratio
t : staying time of falling film along tube [s]
u_L : average flow velocity of falling film [m/s]
V : slurry bulk for absorbing sulfur dioxide [m^3]
V_{in} : flue gas velocity at inlet [m/s]

Greek Letters

δ : average thickness of falling film [m]
η : desulfurization efficiency of reactor, dimensionless

Subscripts

BL : liquid bulk
G : gas phase
i : interface
in : inlet of reactor
L : liquid bulk
out : outlet of reactor
R : reaction layer

REFERENCES

1. H. Zhang, Q. He, Z. Y. Chen and Y. L. Chen, *Electric Power Environmental Protection*, **1**, 21 (2005).
2. X. M. Li and C. L. Jiang, *Coal Technology*, **111**, 24 (2005).
3. Y. W. Nam and K. S. Park, *Korean J. Chem. Eng.*, **370**, 21 (2004).
4. J. D. Killion and S. A. Garimella, *Int. J. Refrigeration*, **755**, 24 (2001).
5. S. Kiil, M. L. Michelsen and D. J. Kim, *Ind. Eng. Chem. Res.*, **2792**, 37 (1998).
6. W. P. Yan, X. M. Ye and H. T. Li, *J. North China Electric Power University*, **59**, 32 (2005).
7. J. C. Sai, S. H. Wu, H. T. Wang and Y. K. Qin, *J. Engineering for Thermal Energy & Power*, **467**, 18 (2003).
8. H. T. Wang, S. H. Wu, Q. Du and Y. K. Qin, *J. Harbin Institute of Technology*, **715**, 35 (2003).
9. H. T. Wang, S. H. Wu, J. C. Sai and Y. K. Qin, *J. Chemical Industry and Engineering (China)*, **659**, 54 (2003).
10. B. K. Kim, *Korean J. Chem. Eng.*, **29**, 4 (1987).
11. H. G. Nygaard, S. Kiil, J. E. Johnsson, J. N. Jensen, J. Hansen, F. Fogh and D. J. Kim, *Fuel*, **1151**, 83 (2004).
12. T. E. Tan, Y. Z. Jin and Y. S. Luo, *Mass transfer-reaction process*, Zhejiang University Press, Hangzhou (1990).
13. Y. H. Wu, B. Feng, Z. Huang and D. J. Li, *J. Engineering for Thermal Energy & Power*, **284**, 14 (1999).